Communications in Physics, Vol. 31, No. 4 (2021), pp. 369-379
DOI:https://doi.org/10.15625/0868-3166/15560

EFFECT OF GEOMETRICAL PROPERTIES ON LOCALIZED SURFACE PLASMON RESONANCE OF GOLD NANOPARTICLES

LUONG LAM NGUYEN, QUOC TRUNG TRINH, QUANG BAO TU, VAN QUYNH NGUYEN AND THI HONG CAM HOANG†

University of Science and Technology of Hanoi, Vietnam Academy of Science and Technology, 18 Hoang Quoc Viet, Cau Giay, Hanoi, Vietnam

E-mail: †hoang-thi-hong.cam@usth.edu.vn

Received 5 October 2020
Accepted for publication 3 August 2021
Published 16 September 2021

Abstract. *This work presents the simulation of localized surface plasmon resonance (LSPR) properties for two discrete shapes of gold nanoparticle (AuNP) (i.e spherical AuNPs with diameters smaller than 100 nm and triangular AuNPs from 20 nm to 40 nm side length and 8 nm thick). The optical properties of AuNPs have been investigated by using the boundary element method implemented in the MNPBEM toolbox. The dependence of the electric field (E-field) distribution and extinction properties on tunable parameters such asAuNPs size and inter-particle separation, as well as the surrounding medium were investigated showing the sensitivity of upto 270 nm/RIU. Mapping of the confined regions in which a local E-field enhanced (i.e hotspot) was also presented. The simulated results revealed a highly geometry-dependent LSPR property that can be used to guide the design of plasmonic AuNPs-based light-harvesting systems for potential applications such as sensing, photocatalysis, surface-enhanced Raman scattering (SERS) and imaging.*

Keywords: simulation; plasmonic; metallic nanoparticle; nanosphere; nanotriangle.

Classification numbers: 05.45.Pq; 73.20.Mf; 78.20.nb.

I. INTRODUCTION

Nanosized metallic particles known as plasmonic nanoparticles (NPs) have been of great interest due to their ability to efficiently trap photons through localized surface plasmon resonance (LSPR) properties. Classically, when a metallic NP is irradiated by light, the oscillating electric field causes electrons to oscillate coherently. The electric field of the light interacts with free electrons in the NPs, leading to charge separation between free electrons and the part of ionic

cores. The Coulomb repulsion among free electrons acts as a restoring force pushing free electrons to move in the opposite direction. It then results in the collective oscillation of electrons around the NPs [1–3]. In case that the frequency of these confined oscillations matches that of irradiated light, electrons oscillate resonantly with a maximum magnitude, resulting in the occurrence of strong absorption in the visible to the near-IR range, as known LSPR [4]. Thanks to this phenomenon, the interaction between light and matter could be optimized in the confined volume that is below the size of diffraction. The light energy therefore can be concentrated in a tiny volume where the electromagnetic field is greatly enhanced [5]. This interesting phenomenon opens a new efficient technique to extend the capability of using LSPR at the nanoscale over the macroscopic area.

Among noble metals, gold has attracted widespread interest because of its strong extinction part of the dielectric function [6]. For spherical Au nanoparticles (AuNPs), it was found that their plasmon absorption bands are located in the visible region, thus particularly feasible for many applications operating under the excitation of available sources such as lasers and LEDs. Moreover, AuNPs possess unique intrinsic properties, such as biocompatibility, high chemical stability, convenient surface modification with organic and biological molecules. These remarkable behaviors of AuNPs make them a promising candidate for LSPR-based sensing [7–10], the analysis of traced analytes by Surface-Enhanced Raman Spectroscopy (SERS) [11], photothermal therapy [12], light-harvesting applications [13].

For the sensing applications, the mechanism of detection relies on the modulation of LSPR signal recorded, which principally due to the change in size, shape, and reflective index of the surrounding medium around AuNPs. So that, maximizing the modulation of the LSPR signal is a strategy to develop an ultra-highly sensitive surface for sensing application [14, 15]. To do so, SERS sensors based on the different AuNPs-shaped including flower-shape [16], nano-island [17] have widely been developed for the rapid detection of analytes.

Putting two NPs close to each other, the electric field in the tiny gap between them becomes enhanced. This region is thus named hotspot. Light-matter interaction reinforces in this confined region [4, 18–24]. It is therefore expected to improve the sensing performance. Recently, it was experimentally shown the formation of plasmon-induced "hotspots" at NPs vicinity wherein the electric field was found to strongly localize [1, 13, 25]. Accordingly, it is crucial to have a systematical investigation of the behavior of this hotspot area at various light wavelengths, inter-particle distances, and the medium surrounding the particles. To this aim, the simulation approach is considered to be useful because it is feasible for mapping plasmon-enhanced optical near field. This technique allows to visually show the hotspot region. It thus helps to investigate the energy conversion from light to chemical energy [26, 27].

In this paper, we present simulation results for the LSPR characteristics of spherical AuNPs and triangular AuNPs with an average size below 100 nm. The effect of the particles' shape, size as well as the surrounding medium, and the polarization of incident light, the inter-particle separation distance between NPs were examined. The extinction/scattering cross-sections of these AuNPs were numerically calculated to map the plasmon-enhanced electric field region. We also estimated the sensitivity of these AuNPs in the order of several hundred nm/RIU when considering surrounding media of air, water and toluene present their potentials for biosensing applications. The resonance shifts the near-field enhancement of the AuNP dimers were analyzed and presented in this paper. The simulation results would bring a convenient way to decide the optimal parameters for the fabrication process of these AuNPs.

II. PLASMON EXCITATION ON SPHERICAL GOLD NANOPARTICLES

II.1. Effect of size on the plasmonic behavior of single spherical gold nanoparticles

For spherical metallic NPs with a size much smaller than the wavelength of light, the Mie solution to Maxwell's equations can be used to describe the light absorption caused by LSPR [5, 28]. According to the Mie theory, for well-separated spherical NPs with a volume V, the extinction cross-section, C_{ext}, can be expressed as

$$C_{\text{ext}} = \frac{18\pi V \varepsilon_{\text{m}}^{3/2}}{\lambda} \frac{\varepsilon_{\text{i}}}{(\varepsilon_{\text{r}} + 2\varepsilon_{\text{m}})^2 + \varepsilon_{\text{i}}^2}, \tag{1}$$

and the scattering cross-section

$$C_{\text{sca}} = \frac{32\pi^4 V^2 \varepsilon_{\text{m}}^2}{\lambda^4} \frac{(\varepsilon_{\text{r}} - \varepsilon_{\text{m}})^2 + \varepsilon_{\text{i}}^2}{(\varepsilon_{\text{r}} + 2\varepsilon_{\text{m}})^2 + \varepsilon_{\text{i}}^2}, \tag{2}$$

where ε_{m} is the dielectric constant of the surrounding medium, ε_{r} and ε_{i} are a real and an imaginary part of the dielectric function of the metallic NPs, respectively. As indicated by equation (1) and (2), the plasmon absorption band appears when $\varepsilon_{\text{r}} = -2\varepsilon_{\text{m}}$ and the color of the spherical NP is observed accordingly.

Here, different sized spherical AuNPs are excited by x-polarized light with wavelength varying from 400 nm to 800 nm in the surrounding medium of air in order to examine their optical response by calculating the extinction cross-section. The calculated extinction (scattering and absorption) cross-section of spherical AuNPs with a diameter in the range of 30 nm to 100 nm as a function of incident light wavelength is depicted in Fig. 1 (a). It is well noted that the extinction cross section increases with respect to the increase of the particle's size, which follows Eq. (1) or Mie theory [5, 28]. In addition, the extinction peak wavelength shifts to the longer wavelength, while the full width at half maximum is broader when the diameter of the particle increases because of the electromagnetic wave retardation [29, 30].

Figure 1(b) presents the electric field distribution of the isolated spherical AuNP with a diameter of 80 nm illuminated by the extinction peak wavelength, *i.e.* 548 nm wavelength x-polarized light. The field enhancement is localized around the particle and is strongly distributed in the x-direction corresponding to the x-polarized incident light. The x-component of the electric field shown in Fig. 1(c) also exhibits the dominant localization along with the light polarization. Therefore, the tight localization of the electric field induced by LSPR makes AuNPs highly sensitive to the small change in the surrounding refractive index.

Figure 2 exhibits the optical responses of the spherical AuNPs with a diameter in the range of 10 nm to 100 nm, being excited by x-polarized light in different surrounding media, *i.e.* air (black solid curve with diamonds), water (red dotted curve with circles), and toluene (blue dashed curve with triangles). In a particular medium, the resonant scattering peak increases linearly with the size of spherical AuNPs, the same behavior of the extinction depicted in Fig. 1. Besides, the scattering peak shifts to longer wavelength as the refractive index of the surrounding medium increases from the air ($n = 1$) to water ($n = 1.344$) and toluene ($n = 1.49$). The sensitivity ($S = \frac{d\lambda}{\text{d}n}$) can be estimated of several hundred nm/RIU, *i.e.*, at approximately 160 nm/RIU for the 80 nm diameter spherical AuNPs. This redshift is attributed to the delayed plasmon resonance [31]. Moreover, the bigger the spherical AuNP, the greater sensitivity to the immersing environment,

this performance is in good agreement with previous observation [32]. This property of spherical AuNPs is the basis for biosensing applications.

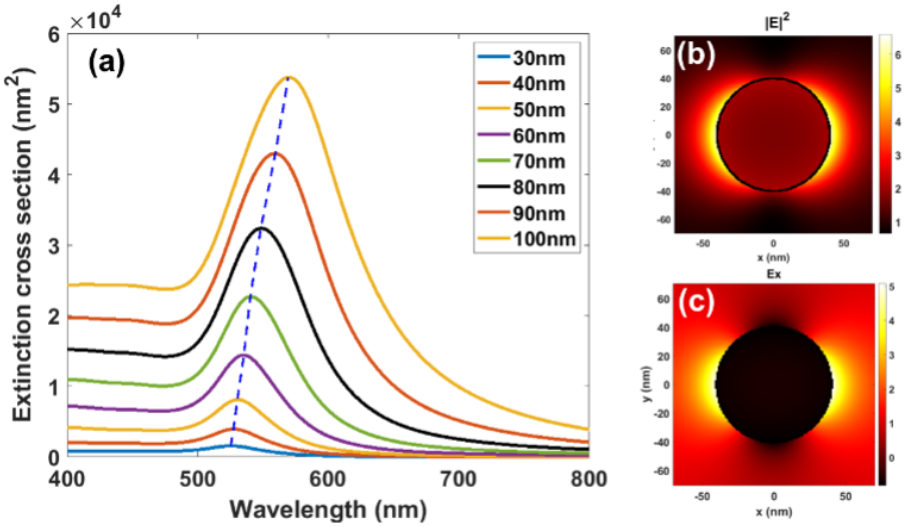

Fig. 1. (Color online) (a) Extinction cross section for different spherical AuNPs with diameter ranging from 30 nm to 100 nm excited by *x*-polarized light in the range of 400-800 nm wavelength, Distribution of (b) electric field magnitude and (c) *x*-component of the electric field for an 80 nm diameter spherical AuNPs excited by a 548 nm *x*-polarized light in the surrounding medium of air.

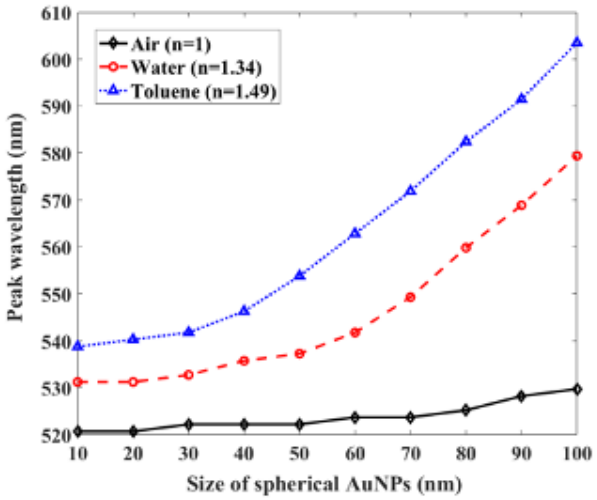

Fig. 2. Evolution of peak wavelength of scattering effect for different size of spherical AuNPs with diameter ranging from 10 nm to 100 nm in the surrounding medium of air (black solid curve with diamonds), water (red dotted curve with circles) and acetone (blue dashed curve with triangles).

II.2. Effect of light polarization and inter-particle separation on the plasmonic behavior of spherical gold nanoparticle dimers

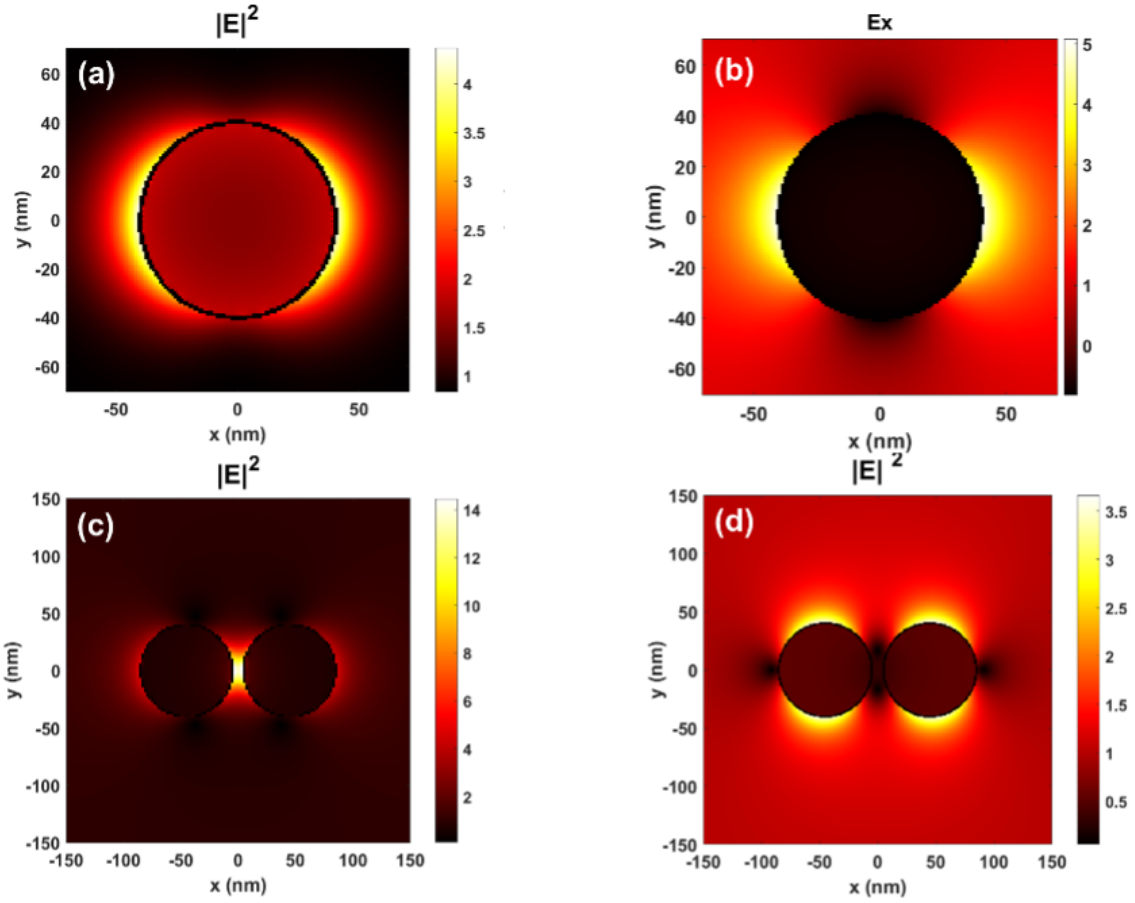

Fig. 3. (a) Electric field distribution and (b) *x*-component of electric field for a spherical AuNP excited by a 650 nm *x*-polarized light. Electric field distribution of a spherical AuNP dimer excited by a 650 nm (c) *x*-polarized light, (d) *y*-polarized light in the surrounding medium of water. The diameter of the spherical AuNP is 80 nm and the inter-particle separation is 10 nm.

When two spherical AuNPs are in the vicinity, the E-field is confined in the gap of the dimer and the polarization of incident light determines the orientation of the field strength. Here, 80 nm diameter spherical AuNPs immersed in water are injected by a 650 nm wavelength light in different polarizations. Figures 3(a) and 3(b) show the distribution of electric field magnitude and the *x*-component electric field of a single spherical AuNP excited by a 650 nm wavelength *x*-polarized light. The electric field profiles obviously align along the *x*-polarization of light with lower intensity compared with those excited by a 548 nm wavelength (the peak wavelength) as depicted in Figs. 1(b) and 1(c). Due to the radial symmetry of the sphere, the polarized light excitation has no effect on the induced electric field strength. Whereas the polarized light has strong influence on both the orientation and the strength of the induced electric field in the spherical AuNP dimer.

Figs. 3(c) and 3(d) present the electric field distribution of the spherical AuNP dimer excited by *x*-polarized and *y*-polarized lights in which the inter-particle separation between two AuNPs is of 10 nm.

The difference in electric field distribution for two light polarizations is caused by the direction of localized oscillation of conduction electrons. In the case the incident light is *x*-polarized, the conduction electrons only oscillate and generate the induced electric field on the two sides of the particles parallel to the *x*-axis (as depicted in Figs. 3(a), 3(b)). When the distance between two isolated spherical AuNPs decreases to a specific distance, the E-field induced satisfies the interference condition, which results in the creation of"hotspot", *i.e.* the region where the electric field is strongly enhanced. The E-field intensity at the"hotspot" is much larger than that of isolated spherical AuNPs. On the other hand, with the irradiation of *y*-polarized light, the E-field formed around the AuNP dimer distributes mainly parallel to the *y*-axis (as shown in Fig. 3(d)). This result thus demonstrates the dependence of the plasmonic properties of these spherical AuNPs on the incident light polarization.

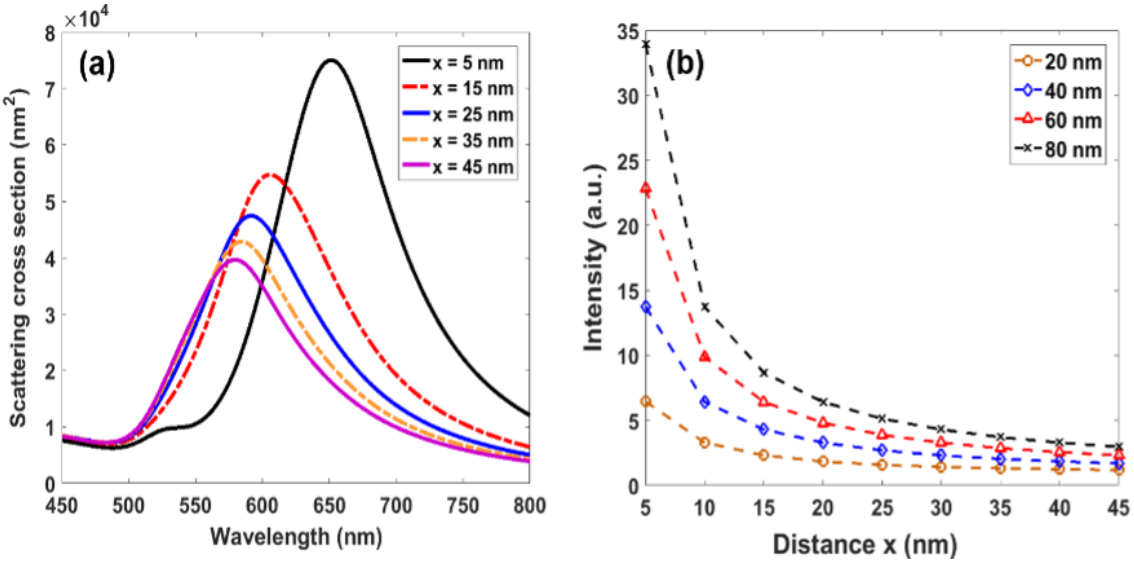

Fig. 4. (a) Scattering cross section for an 80 nm spherical AuNP dimer as a function of the inter-particle separation *x*: $x = 5$ nm (black solid curve), $x = 15$ nm (red dash-dotted curve), $x = 25$ nm (blue solid curve), $x = 35$ nm (yellow dash-dotted curve), $x = 45$ nm (violet solid curve) (b) The dependence of"hotspot" intensity on the inter-particle separation for different size of spherical AuNPs from diameter of 20 nm to 80 nm, excited by the 650 nm wavelength *x*-polarized light in the surrounding medium of water.

Figure 4(a) presents the scattering cross section of an 80 nm diameter spherical AuNP dimer while varying the inter-particle separation between two NPs from 5 nm to 45 nm. The blueshift of scattering peak wavelength and the decrease of scattering cross section are observed as the inter-particle separation increases. This may result from the weaker interaction between the two spherical AuNPs when they get further to each other. As the two AuNPs come closer to each other, the conduction electrons near each particle surface become delocalized and are shared amongst the

neighboring particles. At this state, the scattering peak shifts to longer wavelengths. In order to examine properly the critical inter-particle distance, the intensity of the E-field at the "hotspot" as a function of the inter-particle separation has been investigated and is depicted in Fig. 4(b).

Figure 4(b) describes the evolution of the intensity of the"hotspot" of the spherical AuNP dimer with a diameter ranging from 20 nm to 80 nm as a function of the inter-particle separation from 5 nm to 45 nm, excited by the 650 nm wavelength x-polarized light. The"hotspot" intensity of these spherical AuNP dimers decreases dramatically in the range of 5 nm to 15 nm and slowly decreases until the inter-particle distance is 45 nm. When the two spherical AuNPs are quite close, *e.g.*, 5 nm, the incident light excites the oscillation of conduction electrons which generates the intrinsic induced electric field and it also forms the optimal condition for electrons to tunnel across the region between two AuNPs. However, when the inter-particle separation gets larger, the induced electric field of these spherical AuNPs can't interfere anymore thus the"hotspot" intensity decays. When the inter-particle separation is larger than 15 nm, *i.e.*, the critical distance, the"hotspot" intensity becomes saturated. This result indicates that the two 80 nm diameter spherical AuNPs now become isolated when the inter-particle separation reaches 15 nm. In this situation, the electric field in the region between two NPs is not enhanced by the interference of the induced electric field of each NP. Besides, the larger the size of spherical AuNPs, the higher the intensity of the "hotspot" which can be explained by the larger amount of the conduction electrons in corresponding spheres. The evolution tendency of the"hotspot" intensity in the two spherical AuNPs depends on the size of the NPs. The "hotspot" intensity has steeper slope for larger NPs, however, when the inter-particle separation is beyond the critical distance, the size has negligible effect and the"hotspot" intensity becomes small and similar for different sizes of AuNPs.

III. PLASMON EXCITATION ON TRIANGULAR GOLD NANOPARTICLES

III.1. Plasmonic behavior of single triangular gold nanoparticles

In order to evaluate the shape effect on the plasmonic behavior of AuNPs, we report here the optical response of the single equilateral triangular AuNPs or nanoprisms in different environments. The considered equilateral triangular AuNPs have the side length in the range of 20 nm to 40 nm while the thickness is chosen at 8 nm. Fig. 5(a) depicts the evolution of scattering peak wavelength of these AuNPs excited by x-polarized in air ($n = 1$), water ($n = 1.34$) and toluene (n = 1.49). When the side length increases, *i.e.* the size of NPs gets bigger, the scattering peak wavelength also shifts to the longer range. In addition, the redshift of the LSPR occurs when the refractive index of surrounding medium increases linearly in the same manner as observed in the case of spherical AuNPs. The sensitivity can be extracted up to 270 nm/RIU, these results thus reveal the potential of exploiting these triangular NPs for sensing application.

The dependence of the plasmonic behaviors of these triangular AuNPs on the polarization of incident light is demonstrated in Figs. 5(b)-5(e). Fig. 5(b) presents the E-field distribution of the 30 nm side length and 8 nm thickness equilateral triangular AuNPs excited by a 650 nm x-polarized light in water. In this case, the field is reinforced at the edge of the AuNP as shown by the x-component electric field distribution in Fig. 5(c). While the induced filed is enhanced surrounding two edges along y-axis if the excited light is y-polarized as shown in Fig. 5(d) for the electric field distribution and Figure 5(e) for the x-component profile of the electric field. As the light polarization changes from x-polarized to y-polarized, the magnitude of the electric field in

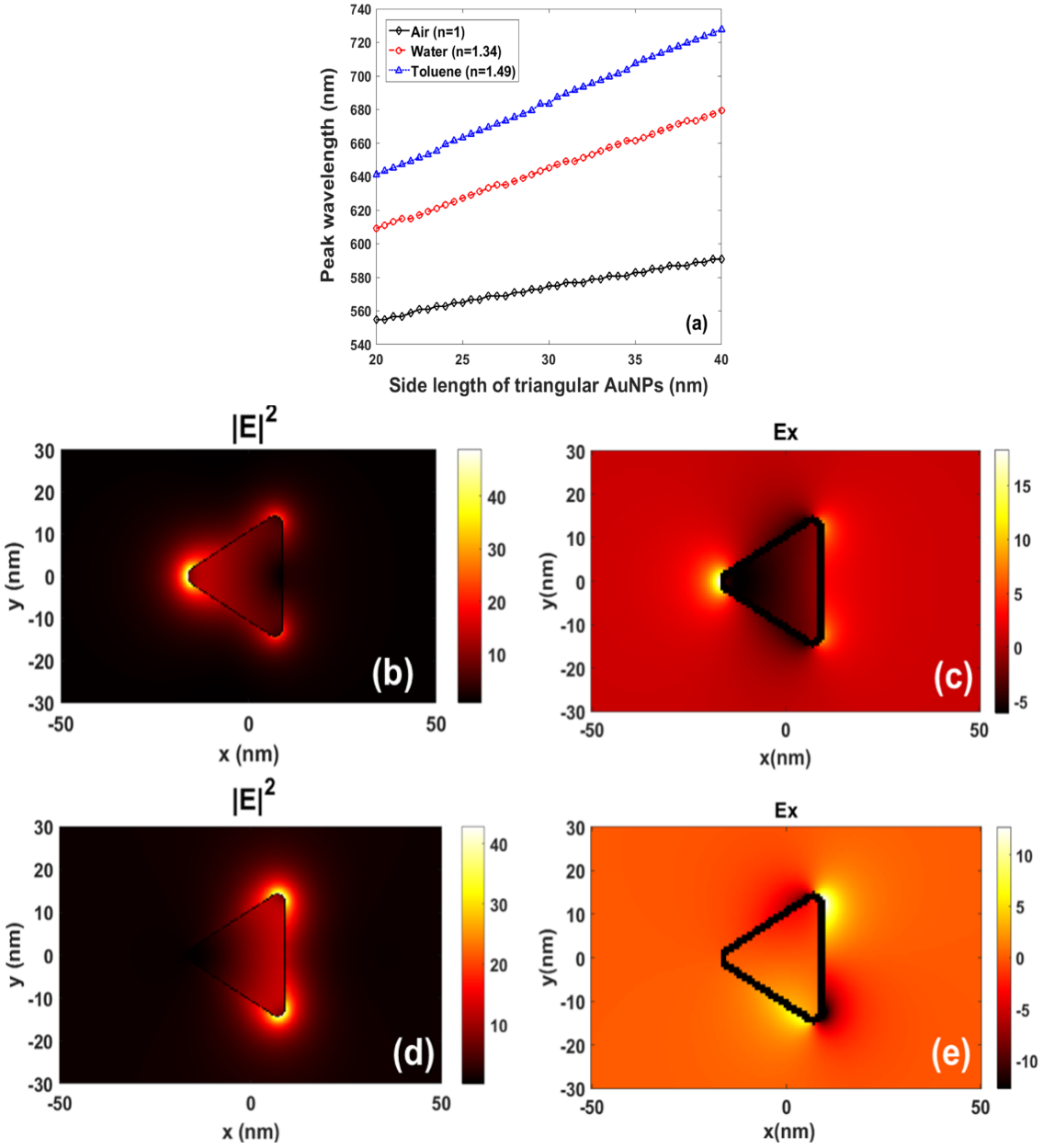

Fig. 5. (a) Evolution of peak wavelength of scattering effect for different size of equilateral triangular AuNPs with size length ranging from 20 nm to 40 nm while the thickness is fixed at 8 nm in the surrounding medium of air (black solid curve with diamonds), water (red dash-dotted curve with circles) and toluene (blue dashed curve with triangles). (b) Electric field distribution and (c) x-component of electric field of a 30 nm side length and 8 nm thickness equilateral triangle excited by a 650 nm x-polarized light and (d) Electric field distribution and (e) x-component of electric field by y-polarized light in water.

x-component decreases. The electric field profile of the AuNPs depends on their shape and here in this triangular AuNPs, the induced electric field is strongly confined around the edges due to the appearance of the sharpness in the triangular AuNPs resulting in the generation of lightning rod effect.

III.2. Effect of gap distance on the plasmonic behavior of triangular gold nanoparticle dimers

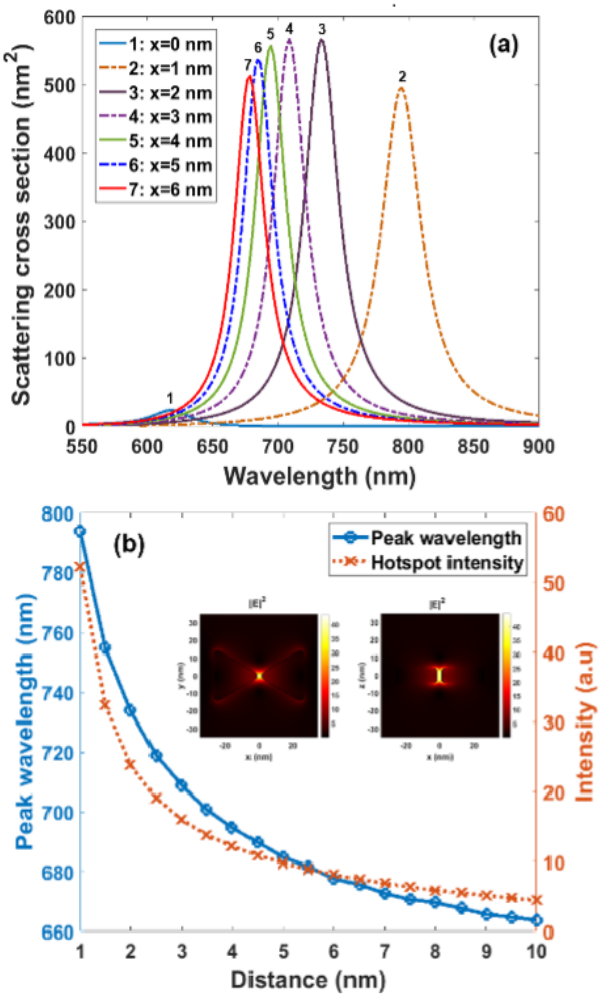

Fig. 6. (a) Scattering cross section for different gap distances between triangular AuNP dimers (side length 30 nm, thickness 8 nm); (b) The evolution of scattering peak wavelength of these triangular AuNP dimers (blue curve) and of the"hotspot" intensity (red curve) as a function of gap distance between AuNPs varying from 1 to 10 nm excited by a 650 nm wavelength *x*-polarized light in water. Insets are the electric field distribution of the 30 nm side length and 8 nm thickness equilateral triangular AuNP dimer with the gap distance of 2 nm in water.

Figure 6(a) depicts the scattering cross section of the 30 nm side length and 8 nm thickness equilateral triangular AuNP dimers for different gap distances between two NPs ranging from

0 nm to 6 nm in the bowtie configuration. These equilateral triangular AuNPs are excited by a 650 nm wavelength *x*-polarized light in water. As the two triangular AuNPs are close enough, the"hotspot" occurs as a result of the interference of the induced electric field of each NPs as well as the lightning rod effect. The scattering peak wavelength is blue-shifted as the gap distance (tip-to-tip) increases. Especially, when the two triangular AuNPs are in contact, or the gap distance is 0 nm, the abnormal spectrum (blue curve) occurs due to the fact that the two triangular AuNPs are now considered as one bowtie NP.

Figure 6(b) reports the dependence of the scattering peak wavelength (blue curve) and the evolution of intensity of the"hotspot" (red curve) on the distance between the two NPs, inset shows the electric field distribution of the triangular AuNP dimer with the gap distance of 2 nm in *xy* plane and *xz* plane. As the gap distance increases, the scattering peak wavelength and the intensity of the"hotspot" decrease, both observations are consistent with previous descriptions of noble triangular nanoprisms [20]. The scattering peak wavelength decreases from approximately 800 nm down to 660 nm when the inter-particle distance continues increase from 1 nm to 10 nm. In the same manner, the"hotspot" intensity decreases exponentially when the separation distance between two triangular AuNPs increases. Moreover, the saturation of intensity when the gap distance is larger than 6 nm exhibits that the two triangular AuNPs become isolated. It can be explained due to the fact that in the bowtie triangular AuNP dimer, the"hotspot" is also affected by the lightning rod effect.

IV. CONCLUSION

We simulated successfully the LRPR of the AuNPs in different geometrical shapes that immersed in different mediums (air, water and toluene) by boundary element method (MNPBEM toolbox). Two configurations including single AuNP and AuNPs dimers with different inter-particle distances have been studied. The diameters of considered spherical AuNPs are smaller than 100 nm while the equilateral triangular AuNPs have side length ranging from 20 nm to 40 nm and the thickness of 8 nm. The simulated results demonstrate the feasibility of AuNPs for the refractive index sensing in which the sensitivity of 160 nm/RIU (for 80 nm diameter spherical AuNPs) and up to 270 nm/RIU (triangular AuNP dimers) has been predicted. The effect of the polarization of the excitation light on the induced electric field in these AuNPs has also been investigated. The blue shift of the scattering peak wavelength and the exponential decrease of the"hotspot" intensity as the inter-particle distance increases in the spherical/triangular AuNP dimers have observed. The achieved results provide the guidelines to design AuNPs-based plasmonic surface for desired applications.

ACKNOWLEDGMENTS

This research is funded by University of Science and Technology of Hanoi (USTH), Vietnam Academy of Science and Technology (VAST) under grant number USTH.NANO.01/18-19.

REFERENCES

[1] V-Q. Nguyen, Y. Ai, P. Martin and J-C. Lacroix, *ACS Omega* **2** (2017) 1947.
[2] J. R. Krenn, G. Schider, W. Rechberger, B. Lamprecht and A. Leitne, *Appl. Phys. Lett.* **77** (2000) 3379.
[3] V. Myroshnychenko, J. Rodríguez-Fernández, I. Pastoriza-Santos, A. M. Funston, C. Novo, P. Mulvaney, L. M. Liz-Marzán and F. J. García de Abajo, *Chem. Soc. Rev.* **37** (2008) 1792.

[4] B. Grześkiewicz, K. Ptaszyński and Michał Kotkowiak, *Plasmonics* **9** (2014) 607-614.
[5] K. M. Mayer and J. H. Hafner, *Chem. Rev.* **111** (2011) 3828.
[6] J. Olson, S. Dominguez-Medina, A. Hoggard, L-Y. Wang, W-S. Chang and S. Link, *Chem. Soc. Rev.* **44** (2015) 40.
[7] J. N. Anker, W. P. Hall, O. Lyandres, N. C. Shah, J. Zhao and R. P. Van Duyne, *Nat. Mat.* **7** (2008) 442.
[8] N. Félidj, J. Grand, G. Laurent, J. Aubard and G. Lévi, *J. Chem. Phys.* **128** (2008) 094702.
[9] Reid E. Messersmith, Greg J. Nusz and Scott M. Reed, *J. Phys. Chem. C.* **117** (2013) 26725.
[10] R. Morarescu, H. Shen, R. A. L. Vallée, B. Maes, B. Kolarica and P. Damman, *J. Mater. Chem.* **22** (2012) 11537.
[11] P. L. Stiles, J. A. Dieringer, N. C. Shah and R. P. Van Duyne, *Annu. Rev. Anal. Chem* **1** (2008) 601.
[12] Xiaohua Huang and M. A. El-Sayed, *J. Adv. Res.* **1** (2010) 13.
[13] S. Kuwahara, Y. Narita, L. Mizuno, H. Kurotsu, H. Yoshino and M. Kuwahara, *ACS Appl. Nano Mater.* **3** (2020) 5172.
[14] J. Cao, T. Suna and K. T. V. Grattan, *Sens. Actuators B* **195** (2014) 332.
[15] Y. Hong, Y-M. Huh, D. S. Yoon and J. Yang, *J. Nanomat.* **2012** (2012) 759830.
[16] N. T.-Q. Luong, D. T. Cao, C. T. Anh, K. N. Minh, N. N. Hai and L. V. Vu,"Electrochemical Synthesis of Flower-Like Gold Nanoparticles for SERS Application," *J. Electron. Mater.* **48** (2014) 5328.
[17] O. T. T. Nguyen, D. Tran, Q. N. Nguyen, N. X. Nguyen, L. H. Nghiem, T. D. Dao, T. Nagao and C. V. Hoang, *Mater. Trans.* **59** (2018) 1081.
[18] Y. B. Zheng, B. K. Juluri, X. Mao, T. R. Walker and Tony Jun Huang, *J. Appl. Phys.* **103** (2008) 014308.
[19] T-R. Lin, S-W. Chang, S. L. Chuang, Z. Zhang and P. J. Schuck,
[20] D. A. Rosen and A. R. Tao, *ACS Appl. Mater. Inter.* **6** (2014) 4134.
[21] H. B. Jeon, P. V. Tsalu and J. W. Ha, *Sci. Rep.* **9** (2019) 13635.
[22] M. Kotkowiak, B. Grześkiewicz, E. Robak and E. Wolarz, *J. Phys. Chem. C.*, (2015) DOI: 10.1021/jp512220e
[23] A. Azarian and F. Babaei, *J. Appl. Phys.* **119** (2016) 203103.
[24] K. L. Shuford, M. A. Ratner and G. C. Schatz, *ACS Appl. Chem. Phys.* **123** (2005) 114713.
[25] T. B. Pham, T. H. C. Hoang, V. H. Pham, V. C. Nguyen, T. V. Nguyen, D. C. Vu, V. H. Pham and H. Bui, *Sci. Rep.* **9** (2019) 12590 DOI: 10.1038/s41598-019-49077-1
[26] S. Dodson, M. Haggui, R. Bachelot, J. Plain, S. Li and Q. Xiong, *J. Phys. Chem. Lett.* **4** (2013) 496.
[27] P. Pavaskar, J. Thesis and S. B. Cronin, *Opt. Express* **20** (2012) 14656.
[28] C. F. Bohren and D. R. Huffman,"Absorption and Scattering of Light by Small Particles, Willey-VCH, Germany, 1998.
[29] K. E. Fong and L-Y. L. Yung, *Nanoscale* **2013** (2013) 12043 DOI: 10.1039/c3nr02257a.
[30] U.Guler and R. Turan, *Opt. Express* **18** (2010) 17322.
[31] S. Pierrat, I. Zins, A. Breivogel and C. Sönnichsen, *Nano. Lett.* **7** (2007) 259.
[32] K-S. Lee and M. A. El-Sayed, *J. Phys. Chem. B* **110** (2006) 19220.